Understanding the Interactions Between the Ocular Surface Microbiome and the Tear Proteome

Denise C. Zysset-Burri,[1,2] Irina Schlegel,[1] Joel-Benjamin Lincke,[1] Damian Jaggi,[1] Irene Keller,[2,3] Manfred Heller,[4] Sophie Braga Lagache,[4] Sebastian Wolf,[1,2] and Martin S. Zinkernagel[1,2]

[1]Department of Ophthalmology, Inselspital, Bern University Hospital, University of Bern, Bern, Switzerland
[2]Department for BioMedical Research, University of Bern, Bern, Switzerland
[3]Interfaculty Bioinformatics Unit and Swiss Institute of Bioinformatics, University of Bern, Bern, Switzerland
[4]Proteomics and Mass Spectrometry Core Facility, Department for BioMedical Research (DBMR), University of Bern, Bern, Switzerland

Correspondence: Denise C. Zysset-Burri, University Hospital Bern, Freiburgstrasse 4, CH-3010 Bern, Switzerland; denise.zysset@insel.ch.

Received: April 30, 2021
Accepted: July 14, 2021
Published: August 9, 2021

Citation: Zysset-Burri Denise C, Schlegel I, Lincke Joel-Benjamin, et al. Understanding the interactions between the ocular surface microbiome and the tear proteome. *Invest Ophthalmol Vis Sci.* 2021;62(10):8. https://doi.org/10.1167/iovs.62.10.8

Purpose. The purpose of this study was to explore the interplay between the ocular surface microbiome and the tear proteome in humans in order to better understand the pathogenesis of ocular surface-associated diseases.

Methods. Twenty eyes from 20 participants were included in the study. The ocular surface microbiome was sequenced by whole-metagenome shotgun sequencing using lid and conjunctival swabs. Furthermore, the tear proteome was identified using chromatography tandem mass spectrometry. After compositional and functional profiling of the metagenome and functional characterization of the proteome by gene ontology, association studies between the ocular microbiome and tear proteome were assessed.

Results. Two hundred twenty-nine taxa were identified with *Actinobacteria* and *Proteobacteria* being the most abundant phyla with significantly more *Propionibacterium acnes* and *Staphylococcus epidermidis* in lid compared to conjunctival swabs. The lid metagenomes were enriched in genes of the glycolysis lll and adenosine nucleotides de novo and L-isoleucine biosynthesis. Correlations between the phylum *Firmicutes* and fatty acid metabolism, between the genus *Agrobacterium* as well as vitamin B1 synthesis and antimicrobial activity, and between biosynthesis of heme, L-arginine, as well as L-citrulline and human vision were detected.

Conclusions. The ocular surface microbiome was found to be associated with the tear proteome with a role in human immune defense. This study has a potential impact on the development of treatment strategies for ocular surface-associated diseases.

Keywords: ocular surface, ocular surface microbiome, whole-metagenome shotgun sequencing, tear proteome, chromatography tandem mass spectrometry

The human microbiome is composed of trillions of bacteria, viruses, and fungi living in and on the human body. In 2007, the Human Microbiome Project characterized the microbiomes at 5 different body sites, including the skin, gastrointestinal tract, oral cavity, nasal passages, and urogenital tract in healthy human subjects, thereby improving the understanding of the microbial flora involved in human health and disease.[1] Under normal physiological conditions, the microbiome is a homeostatic ecosystem with several essential functions. However, disruption of this homeostasis, called dysbiosis, is associated with multiple diseases. In previous studies, we have shown compositional and functional associations of the gut microbiome with several eye diseases, such as age-related macular degeneration[2] and retinal artery occlusion.[3]

However, the surface of the eye has not been studied in the Human Microbiome Project. Thus, the knowledge of the microbial composition in this area, called ocular microbiome, remained limited and still needs more investigation. Although the bacterial colonization of the conjunctiva in healthy subjects has been described early by traditional culturing,[4] these techniques do not allow the identification of the entire bacterial diversity. For example, *Staphylococcus species*, *Corynebacterium species*, and *Propionibacterium acnes* could be cultured from lid margins,[5] indicating the existence of commensal bacteria, but a more in-depth characterization of the microbiome remained a challenge. In the last few years, modern sequencing technologies have allowed a specific bacterial characterization and functional profiling of the ocular microbiome. Using 16s rRNA sequencing, Huang et al. classified bacteria of conjunctival swabs into 25 phyla and 526 distinct genera. The most frequently found phyla were *Proteobacteria, Actinobacteria*, and *Firmicutes* with *Corynebacterium, Propionibacterium, Pseudomonas, Staphylococcus, Streptococcus*, and *Acinetobacter* being the most dominant genera in the

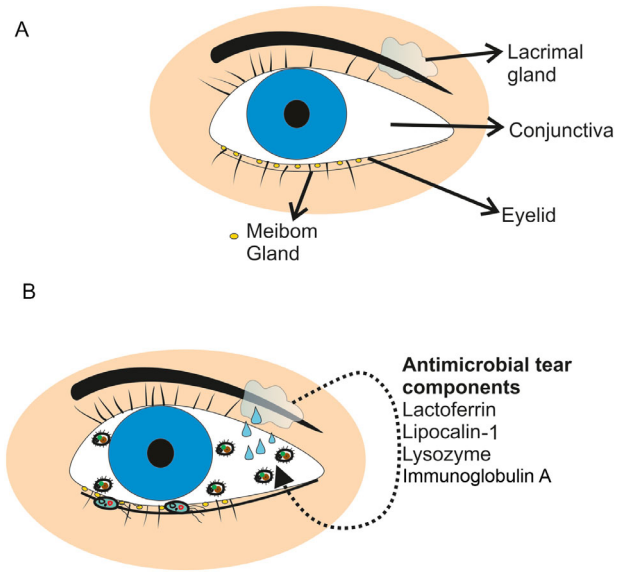

Figure 1. Interactions between the ocular surface microbiome and the tear proteome. The tear film consists of an inner mucin-enriched glycocalyx layer, a middle aqueous layer secreted by lacrimal glands and an outer lipid layer composed of meibomian lipids. Sampling for this study was performed in the following manner: The ocular surface microbiome was sequenced using swabs from the conjunctiva and the eyelid and the tear proteome was characterized collecting tear fluid by Schirmer strips (**A**) (more details are found in section 2.2). Lacrimal constituents of tears may be influenced by the surface microbiome and vice versa through antimicrobial components found in the tear proteome such as lactoferrin, lipocalin-1, lysozyme, and immunoglobulin A (**B**).

eye.[6] In the present study, we taxonomically and functionally characterized the ocular microbiome from conjunctiva and lid through whole-metagenome shotgun sequencing, which allows bacterial as well as viral and fungal profiling and the identification of associated pathways.

In fact, the ocular microbiome harbors a much less diverse variety of species compared to the oral and gut microbiome that may, at least partially, be explained by antimicrobial components in meibomian lipids. Meibomian lipids form a blanket, the lipid layer, covering the middle aqueous layer and the inner glycocalyx layer of human tears (Fig. 1A).[7] In general, the composition of the latter reflects the health of the underlying tissue and, thus, several attempts have been made to explore the human tear proteome to detect potential biomarkers of ocular surface health and disease.[8–11] Applying mass spectrometry using the high speed TripleTOF 5600 system, Zhou et al. have presented a comprehensive list of 1543 proteins that may serve as a reference list of human tear proteome for biomarker discovery.[12] In this study, through nano liquid chromatography tandem mass spectrometry (nLC-MS/MS) we quantified 2172 tear proteins that may extend this list and, furthermore, we functionally classified the tear proteome enabling correlation studies with the profiled microbiome data.

However, although there seems to be a potential interplay between the microbial composition on the ocular surface and proteins in tear fluid with a crucial impact on ocular health and disease, associations between the two systems have not been studied so far. Thus, in this study, we performed association studies between the ocular microbiome and the tear proteome in humans, to set the basis for the identification of potential biomarkers for ocular surface diseases and associated systemic disease states.

Methods

Study Design and Recruitment

This study was approved by the Ethics Committee of the Canton of Bern (ClinicalTrials.gov: NCT04656197). The procedures followed the tenets of the Declaration of Helsinki and the International Ethical Guidelines for Biomedical Research involving Human Subjects (Council for International Organizations of Medical Sciences). After receiving oral and written information, all participants gave written informed consent before study enrollment.

Participants ($n = 20$) aged 60 years or older were consecutively recruited from the Department of Ophthalmology of the University Hospital Bern (Inselspital), Switzerland. Patients with a history of recent (last 3 months) ocular surgery, systemic or topical antibiotics within the last 3 months, as well as smokers and participants wearing contact lenses or using systemic immunomodulators and corticosteroids were excluded. After verifying that no exclusion criteria were met and written informed consent was given, one representative eye was randomly chosen for inclusion.

Sample Collection

Tear fluid was collected by Schirmer's type 2 tear test using one drop of Tetracaine HCL (Tetracaine 1% SDU Faure; Thea Pharma S.A., Schaffhausen, Switzerland) for anesthesia. Three minutes after instillation of Tetracaine HCL, a standard filter strip (Haag-Streit AG, Köniz, Bern, Switzerland) was inserted into the lower conjunctival bag. After 5 minutes, the strip was removed and immediately processed for tear fluid extraction, as described below. Next, a lid swab along the edge of the lid and a swab of the tarsal conjunctiva using a sterile cotton stick (Applimed SA, Châtel-St-Denis, Switzerland) were taken (see Fig. 1A). For negative controls, sterile cotton sticks without ($n = 2$) and with one drop of Tetracaine HCL ($n = 2$), respectively, were processed as lid and conjunctival swabs.

Metagenomic DNA Sequencing and Annotation

Lid and conjunctival swabs as well as negative controls were processed and DNA was isolated at the same day using the E.Z.N.A. MicroELute Genomic DNA kit (Omega Bio-Tek, Inc., Norcross, GA, USA) according to the manufacturer's protocol with an integrated RNA digestion step using 100 mg/mL RNase A (Qiagen, Hombrechtikon, Switzerland). DNA was stored at −20°C until further analysis.

The DNA was brought to the Next Generation Sequencing Platform of the University of Bern, Switzerland, for metagenomics shotgun sequencing. The Nextera DNA Flex Library Preparation kit was used for library preparation for sequencing following standard pipelines of the Illumina NovaSeq 6000 Sequencing System. To exclude low-quality reads and reads mapping to human DNA, the resulting 150 bp paired-end reads were quality filtered using Trimmomatic version 0.32[13] and mapped to the human reference genome hg19 using Bowtie2 version 2.2.4.[14]

Investigative Ophthalmology & Visual Science

For taxonomical annotation, the Metagenomic Phylogenetic Analysis tool version 2.6.0 (MetaPhlAn2) and the marker database version 20[15] were applied with default settings. The relative abundances of each taxonomic unit were calculated using Bowtie2 for alignment followed by normalization of the total number of reads in each clade by the nucleotide length of its marker.

For functional annotation, the Human Microbiome Project (HMP[16]) Unified Metabolic Analysis Network (HUMAnN2 version 0.11.0[17]) was applied with default settings. In order to provide a functional annotation of the taxonomical profiles from MetaPhlAn2, HUMAnN2 was run for each sample separately as described in Zysset-Burri et al.,[3] finally providing a set of pathways including their abundances.

Tear Fluid Collection and Processing

For tear fluid collection, the tear fluid-soaked Schirmer stripe was put into a 0.5 mL Protein LoBind tube (Eppendorg AG, Hamburg, Germany) punctured at the bottom with a cannula. This tube was placed into a larger 2 mL Protein LoBind tube and centrifuged at maximum speed for 5 minutes. This procedure was initially described by Posa et al.[18] and allows the extraction of tear fluid. Tear fluid was stored at −80°C until further analysis by nLC-MS/MS.

Before nLC-MS/MS, 2 µL tear fluid was diluted with 8 µL 8M urea/ 100 mM Tris, reduced for 30 minutes at 37°C with 0.1 M DTT/100 mM Tris, alkylated for 30 minutes in darkness with 0.5 M IAA/100 mM Tris at 37°C and quenched with DTT. The sample was filled up to 20 µL with 6× Laemmli buffer and boiled for 5 minutes at 95°C prior to loading on a 12.5% SDS-PAGE gel. The sample was developed into the gel for about 1.5 cm. Proteins were stained with Coomassie blue, and each lane was cut into five bands of equal size. Gel bands were cut into small cubes, which were transferred to 1.5 mL polypropylene reaction vials and wetted with 100 µL 20% ethanol for storage at 4°C until digestion.

For nLC-MS/MS analysis, the 20 samples were randomized in order to control sample processing bias. Proteins were in-gel digested, as described elsewhere.[19] An aliquot of 5 µL from each digest was analyzed by nLC-MS/MS on an instrumental setup consisting of an EASY-nLC 1000 chromatograph coupled to a QExactive HF mass spectrometer (ThermoFisher Scientific, Reinach, Switzerland). Peptides were trapped on an Acclaim C18 PepMap100 pre-column (5 µm, 100 Å, 300 µm × 5 mm, ThermoFisher Scientific) and separated by backflush on a C18 column (3 µm, 100 Å, 75 µm × 15 cm, Nikkyo Technos, Tokyo, Japan) by applying a 40 minute gradient of 5% acetonitrile to 40% in water, 0.1% formic acid, at a flow rate of 350 nL/min. Peptides of m/z 400 to 1400 were detected at a resolution of 60,000 (at m/z 250) with an automatic gain control (AGC) target of 1E06 and maximum ion injection time of 50 ms. A top 15 data dependent method for precursor ion fragmentation was applied with the following settings: precursor ion isolation width of 1.6 m/z, resolution 15,000, AGC of 1E05, maximum ion time of 110 ms, charge inclusion of 2+ to 7+ ions, peptide match on, and dynamic exclusion for 20 seconds, respectively.

Mass spectrometry data were processed with MaxQuant/Andromeda version 1.6.1.0 using default settings for peak detection, a strict trypsin cleavage rule, allowing up to 3 missed cleavages, variable oxidation on methionine, acetylation of protein N-termini, and deamidation of asparagine and glutamine, and fixed carbamidomethylation of cysteines, respectively. Match between runs was used with a retention time window of 0.7 minutes between neighboring gel fractions but not between samples. The SwissProt human protein sequence database (version 2019_02) was used to interpret fragment spectra with an initial mass tolerance of 10 ppm on precursor and 20 ppm for fragment ions, respectively. Protein identifications were accepted if at least two razor peptides per protein group were identified at a 1% false discovery rate (FDR) cutoff. The across samples normalized MaxQuant calculated protein group LFQ intensities were used to generate protein lists for each sample with proteins divided into up- and downregulated fractions. The median LFQ intensity was used as cutoff for the regulation: if the median LFQ protein group intensity of all samples was smaller than the LFQ value of the protein group of a sample, the protein was considered to be upregulated in the corresponding sample. If the median LFQ protein group intensity of all samples was greater or equal to the LFQ value of the protein group, the protein was considered to be downregulated in the corresponding sample.

Bioinformatic Analysis

To identify differences in microbial and pathway abundances, the Wilcoxon rank sum test was applied. For functional enrichment analysis of up- and downregulated proteins, STRING version 11.0 (https://string-db.org/) was applied using log LFQ values for ranking. The resulting Gene Ontology (GO) terms that were found in at least 80% of all samples were used as metadata for association studies (see below). R software (version 3.6.1) was used to perform other analysis. In order to provide global analysis of microbial and pathway abundances between lid and conjunctival samples by principal component analysis (PCA), the R package *ade4*[20] was applied. PCA was performed using scaled values on relative abundances of microbial species identified by MetaPhlAn2 and of pathways identified by HUMAnN2. A visualization of the individual samples grouped by lid and conjunctiva is provided in Figures 4A and 4B. Permutation multivariate analysis of variance (PERMANOVA) applying the R package *vegan*[21] was assessed with 1000 permutations to provide a P value for separation. Associations of microbial and functional features of the microbiome with functional features of the proteome were identified by multivariate association by linear models (MaAsLin)[22] R package. Significant associations were considered below a q value threshold of 0.40 and $N \neq 0$ in at least 50% of the samples after adjusting for FDR (Benjamini-Hochberg).

Results

Demographic Data

A total of 20 lid and 20 conjunctival swabs as well as tear fluid from 20 eyes of 20 participants were collected. Because both the ocular microbiome[23] and the tear proteome[24] are age-dependent, we included participants aged 60 years or older with a mean of age 69.7 ± 8.3 (SD). Seventy-five percent of study participants were men and 25% were women.

Investigative Ophthalmology & Visual Science

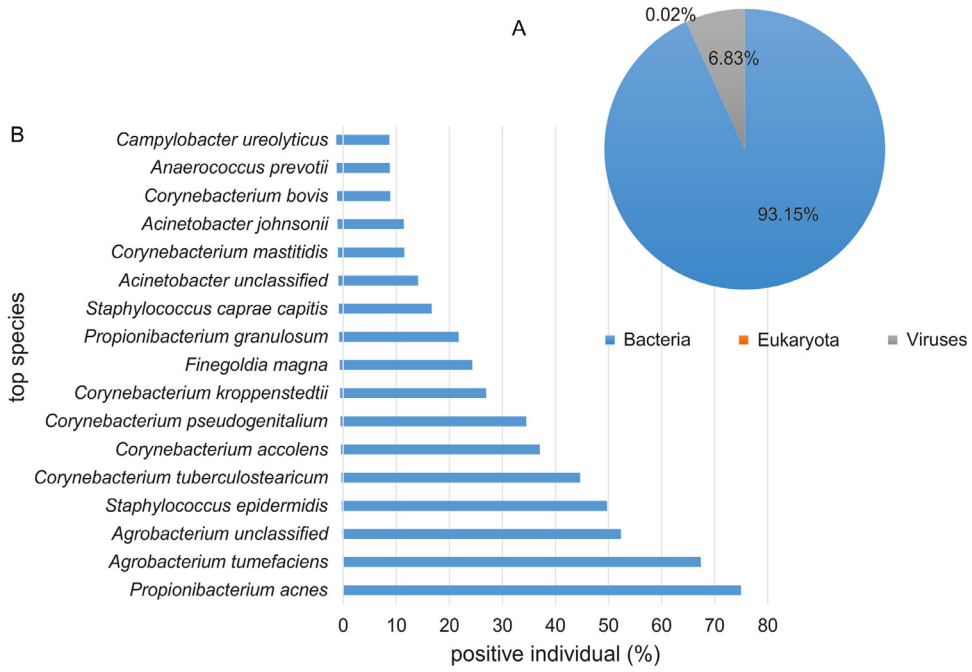

Figure 2. Composition of the ocular surface microbiome. Relative taxonomic composition of the ocular surface microbiome (**A**) and positive rate of species in participants (**B**). The top species with a positive rate ≥ 10% are shown.

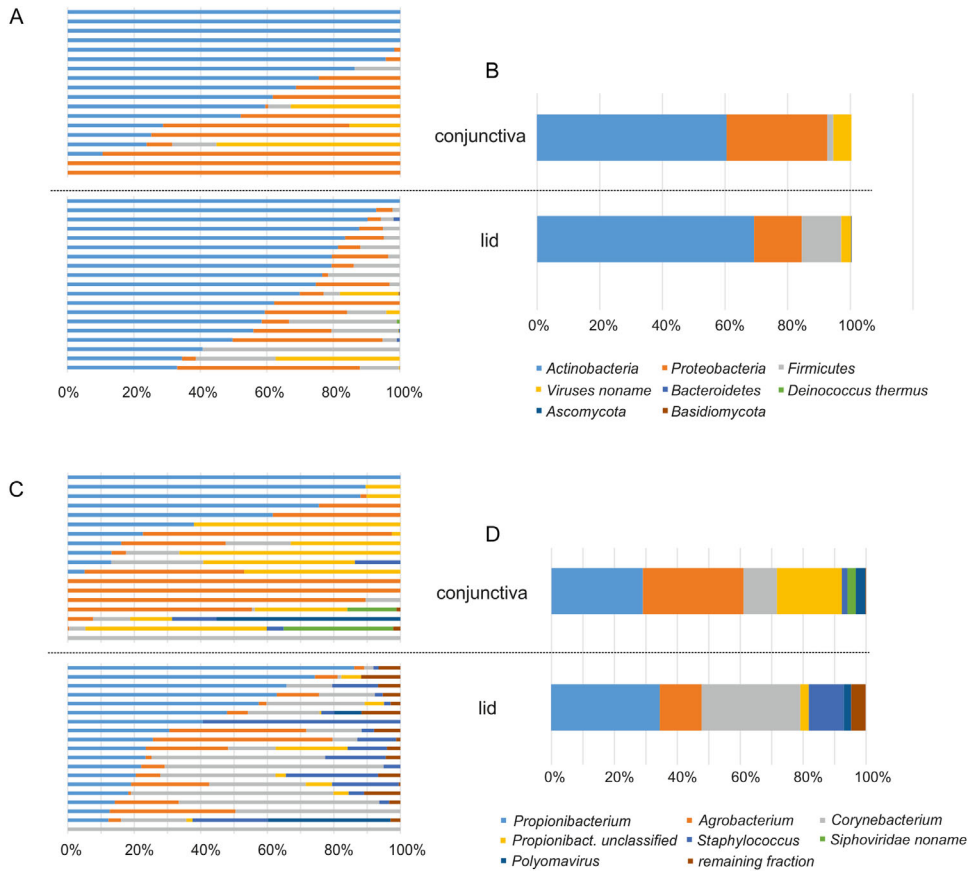

Figure 3. Diversity of the ocular surface microbiome in lid and conjunctival samples. Relative abundances of microbiota at phyla level in individual samples (**A**) and averaged for location (**B**). Relative abundances of microbiota at genus level in individual samples (**C**) and averaged for location (**D**). Conjunctiva $n = 20$ and lid $n = 20$.

Investigative Ophthalmology & Visual Science

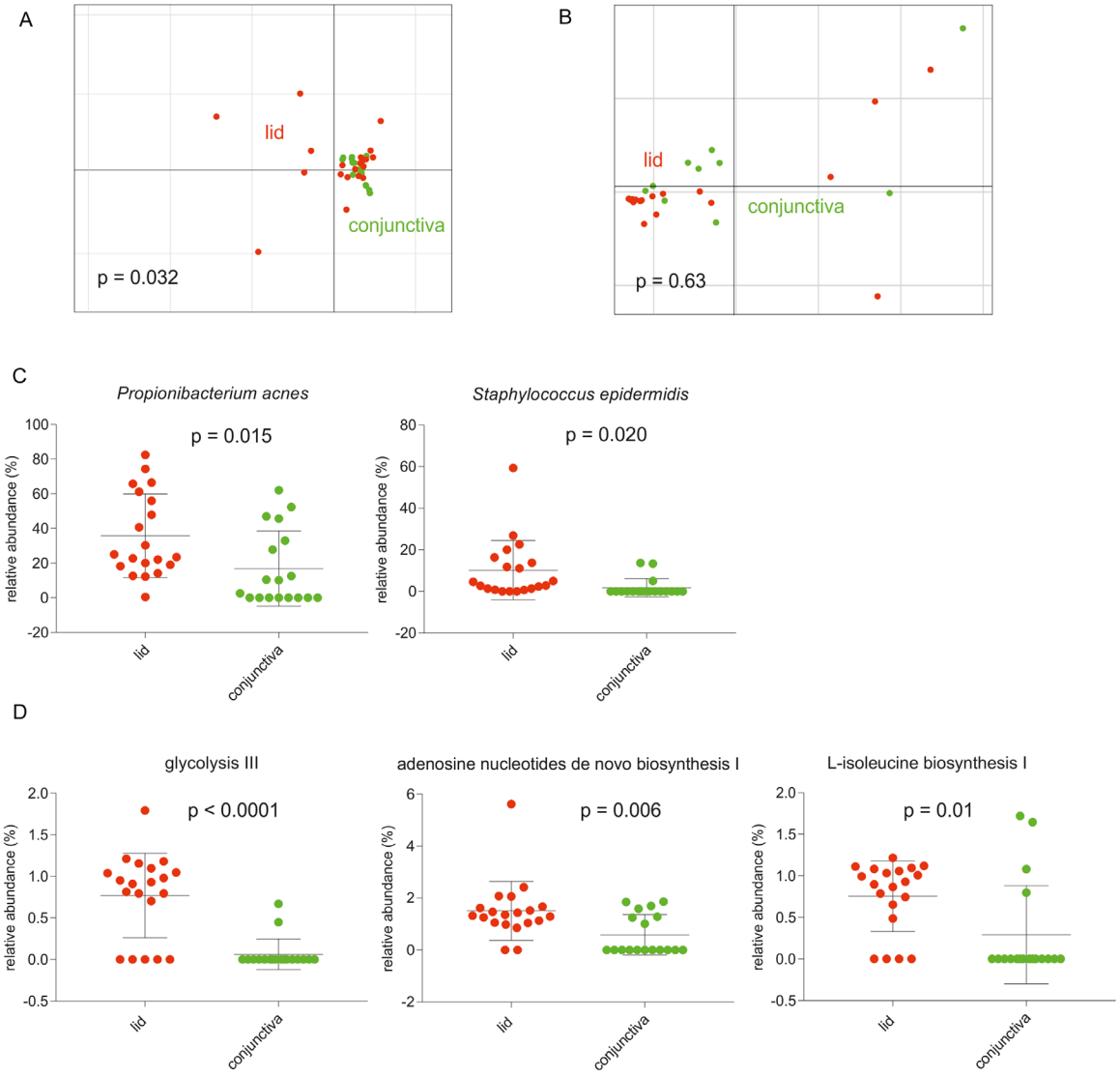

Figure 4. Distinct taxonomical and functional composition of the ocular microbiome between lid and conjunctival samples. Principal component analysis (PCA) of taxonomical feature abundance grouped lid and conjunctival samples separately, with PERMANOVA confirming a significant difference between the groups (**A**) ($P = 0.032$). PCA of functional feature abundance did not separate lid from conjunctival samples (**B**) ($P = 0.63$, PERMANOVA). Relative abundances of taxa (**C**) and pathways (**D**) associated with the location of sampling (mean value and standard deviation are shown, Wilcoxon rank sum test, $P < 0.05$). Red is lid (0 =20), green is conjunctiva $n = 20$.

Taxonomical and Functional Characterization of the Human Ocular Surface Microbiome

The sequencing libraries retrieved from negative controls failed quality and quantity controls for sequencing, ensuring that no contaminations have been sequenced. In total, 1.5 billion 100 bp paired-end reads with an average insert size of 350 bp were generated, with an average of 36.6 ± 7.8 (SD) million reads per sample. As expected, and described in recent studies, the majority of these reads were of human origin. However, after trimming and filtering, we kept about 96.4 million non-human high-quality reads with an average of 2.4 million reads per sample. We identified 229 taxa, the majority of which were bacteria with 93.15%, whereas 6.83% and 0.02% were viruses and eukaryotes, respectively (Fig. 2A). The phyla *Actinobacteria* (64.8%) and *Proteobacteria* (23.4%) dominated the ocular microbiome composition (Figs. 3A, 3B). *Actinobacteria* (63.1%) was the most abundant class, whereas *Propionibacterium* (31.9%), *Agrobacterium* (22.4%), and *Corynebacterium* (21.2%) were the most abundant genera in the cohort (Figs. 3C, 3D). *Propionibacterium acnes* was detected in 75.0% of the samples, and the positive rates for *Agrobacterium tumefaciens, Agrobacterium unclassified*, and *Staphylococcus epidermidis* were 67.5%, 52.5%, and 50.0%, respectively (Fig. 2B).

A PCA using the localization of the swab (lid versus conjunctiva) as grouping variable confirmed that the lid microbiome is separated from the conjunctival microbiome based on differences in taxonomical abundances ($P = 0.032$, PERMANOVA analysis with nrepeat = 10,000; see Fig. 4A). However, the two groups could not be separated according

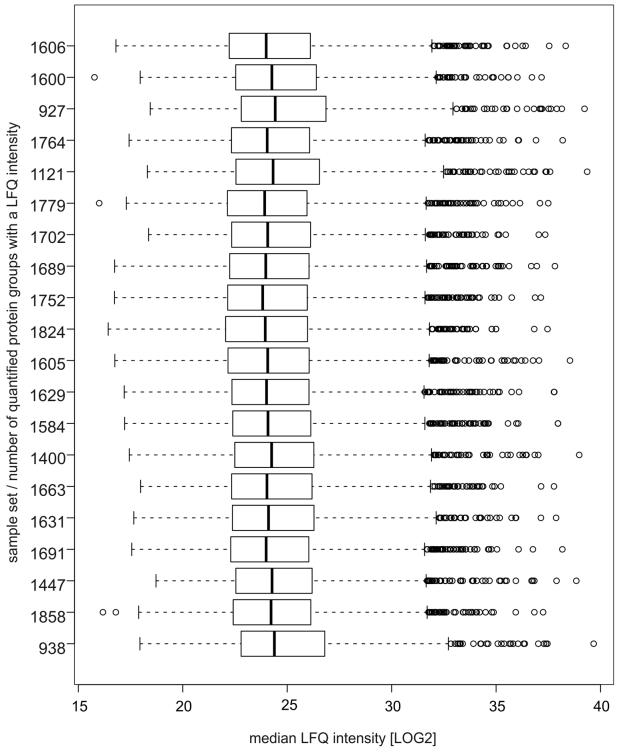

Figure 5. Median label-free quantification (LFQ) protein group intensity of all samples. LFQ intensities of all samples (y-axis) are represented as boxplots. The numbers on the y-axis represent the numbers of quantified proteins with a LFQ intensity. The lines within the boxes delineate median values, the left and right edge of the boxes the 25th and 75th percentiles, the whiskers extend to the most extreme data points, and outliers are represented individually by dots.

to differences in relative abundances of functional profiles (P = 0.63, PERMANOVA analysis wit nrepeat = 10,000; see Fig. 4B). To further examine features of the ocular surface microbiome, we compared the relative abundances of taxa between lid and conjunctival swabs, showing that the two species *Propionibacterium acnes* (P = 0.015) and *Staphylococcus epidermidis* (P = 0.020, Welch's t-test) were more abundant in lid samples (Fig. 4C). Furthermore, lid microbiomes were enriched in genes of glycolysis lll (P < 0.0001), adenosine de novo biosynthesis (P = 0.006) and L-isoleucine biosynthesis pathways (P = 0.01, Welch's t-test; Fig. 4D).

Functional Classification of the Human Tear Proteome

In total, we identified and quantified 2172 protein groups (5392 proteins and 29,129 unique peptides, at 1% FDR) with 594 (27.3%) identified in all samples and a mean of 1561 protein groups per sample (see Fig. 5). Among the 2172 protein groups, 1589 proteins (73.2%) were identified by more than one peptide. Lactotransferrin, albumin, lipocalin-1, lysozyme, and immunoglobulin A were the most abundant proteins in the cohort (Fig. 6A). The mean of the across samples normalized MaxQuant calculated protein group label-free quantification (LFQ) intensities were used as cutoff to generate protein lists for each sample containing up- and downregulated proteins. On average, 963 proteins were considered to be upregulated and 1209 proteins were downregulated (Fig. 6B). Significantly more proteins were downregulated (P = 0.013, unpaired t-test) probably due to the fact that the LFQ value of protein groups that had not been identified in a sample, were set to zero and, therefore, the corresponding protein group was assigned per definition to the downregulated fraction.

Functional classification of identified proteins was done using the DAVID Bioinformatics tool[25,26] based on the GO categories cellular component, biological process, and molecular function (Fig. 7). For cellular component, the top five subcategories are extracellular exosome (20%), cytoplasm (17%), cytosol (17%), nucleus (11%), and membrane (8%; see Fig. 6A). Classification according to

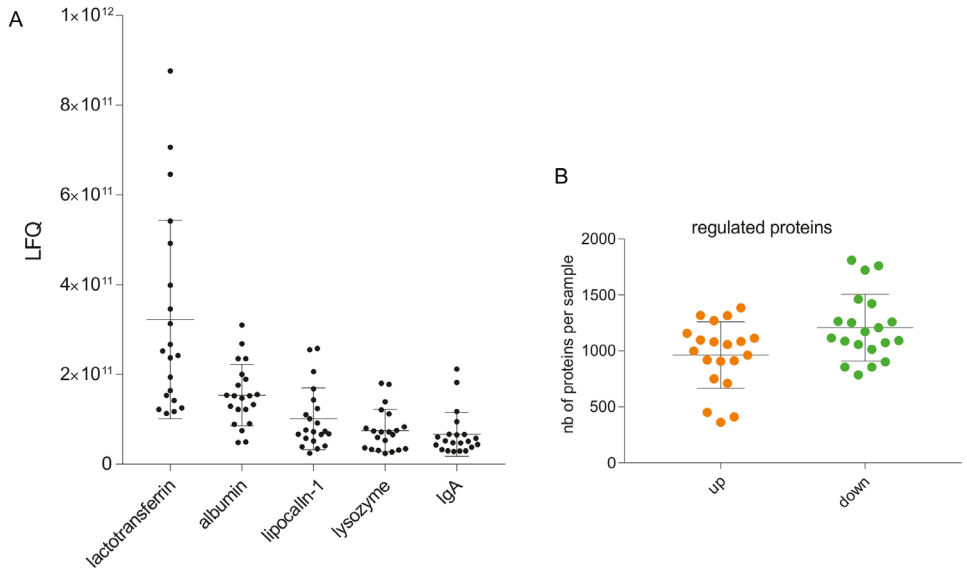

Figure 6. Core proteome of human tears. Label-free quantification (LFQ) values of the most abundant proteins in the cohort (**A**) and the number of regulated proteins per sample (**B**) are represented. There are more downregulated proteins in the cohort (P = 0.013, unpaired t-test). Mean value and standard deviation are shown. IgA, immunoglobulin A; nb, number.

Investigative Ophthalmology & Visual Science

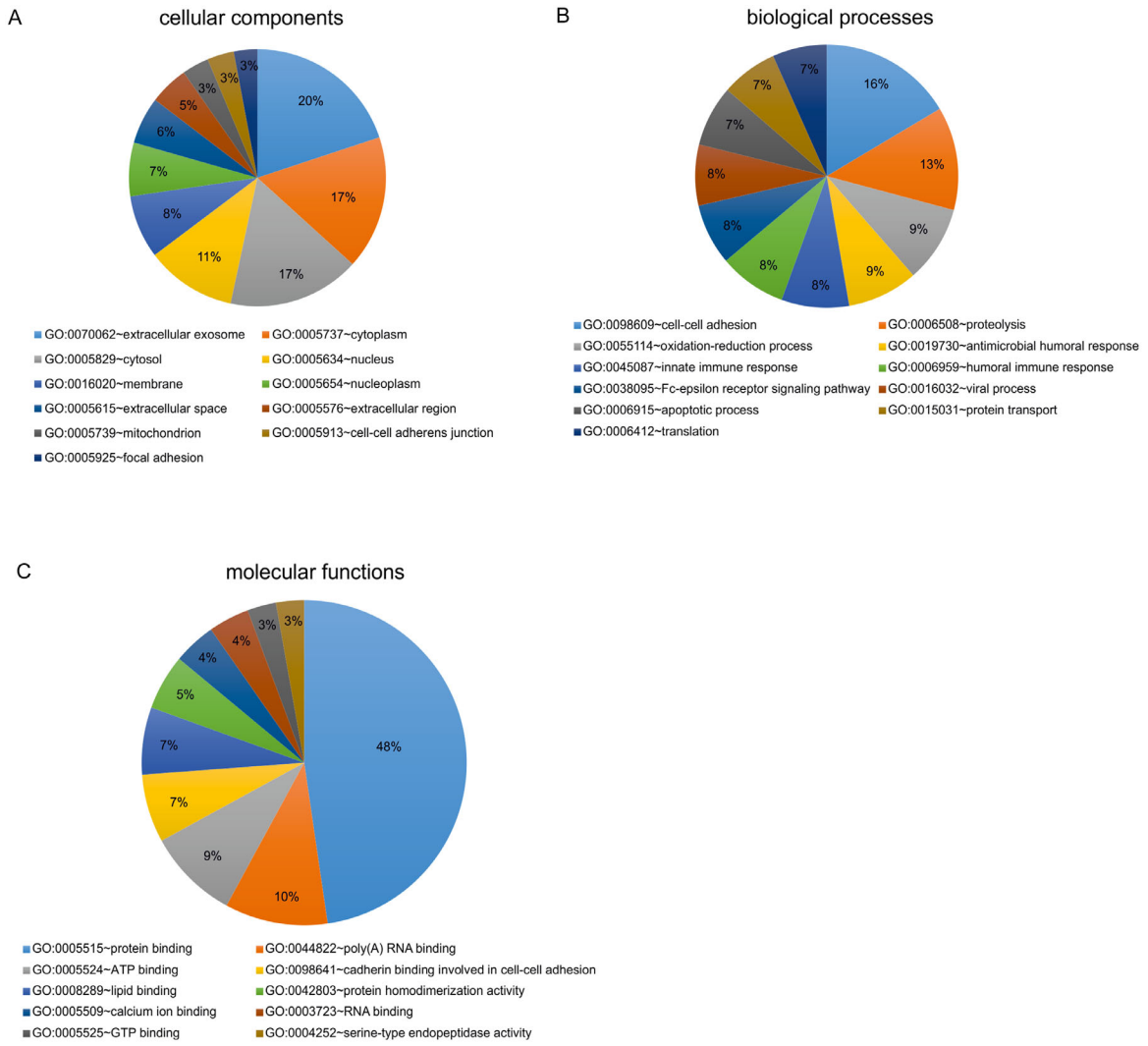

Figure 7. Functional classification of the tear proteome. Classification based on Gene Ontology (GO) categories cellular components (**A**), biological processes (**B**), and molecular functions (**C**) using the DAVID Bioinformatics tool.

Table. Regulated Gene Ontology (GO) Terms

Category	Term ID	Description
Biological process	GO ~ 0007606	Sensory perception of chemical stimulus
Biological process	GO ~ 0019730	Antimicrobial humoral response
Biological process	GO ~ 0019731	Antibacterial humoral response
Molecular function	GO ~ 0005504	Fatty acid binding
Molecular function	GO ~ 0016491	Oxidoreductase activity
Molecular function	GO ~ 0004866	Endopeptidase inhibitor activity

Up- or downregulated GO terms found in at least 80% of all samples.

biological processes revealed that these proteins are mainly involved in cell-cell adhesion (16%), proteolysis (13%), oxidation-reduction process (9%), antimicrobial humoral response (9%), and in innate immune response (8%; see Fig. 6B). For molecular function, most of the proteins are involved in protein binding (48%), followed by poly(A) RNA binding (10%), ATP binding (9%), cadherin binding involved in cell-cell adhesion (7%), and identical protein binding (7%; Fig. 6C).

Associations Between the Human Ocular Surface Microbiome and the Tear Proteome

Based on the up- and downregulated protein lists of each sample, we performed a functional enrichment analysis implemented in STRING[17] using the log LFQ protein group intensities for ranking. The resulting GO terms that had been found in at least 80% of all samples (Table) were used for association studies between the ocular

Investigative Ophthalmology & Visual Science

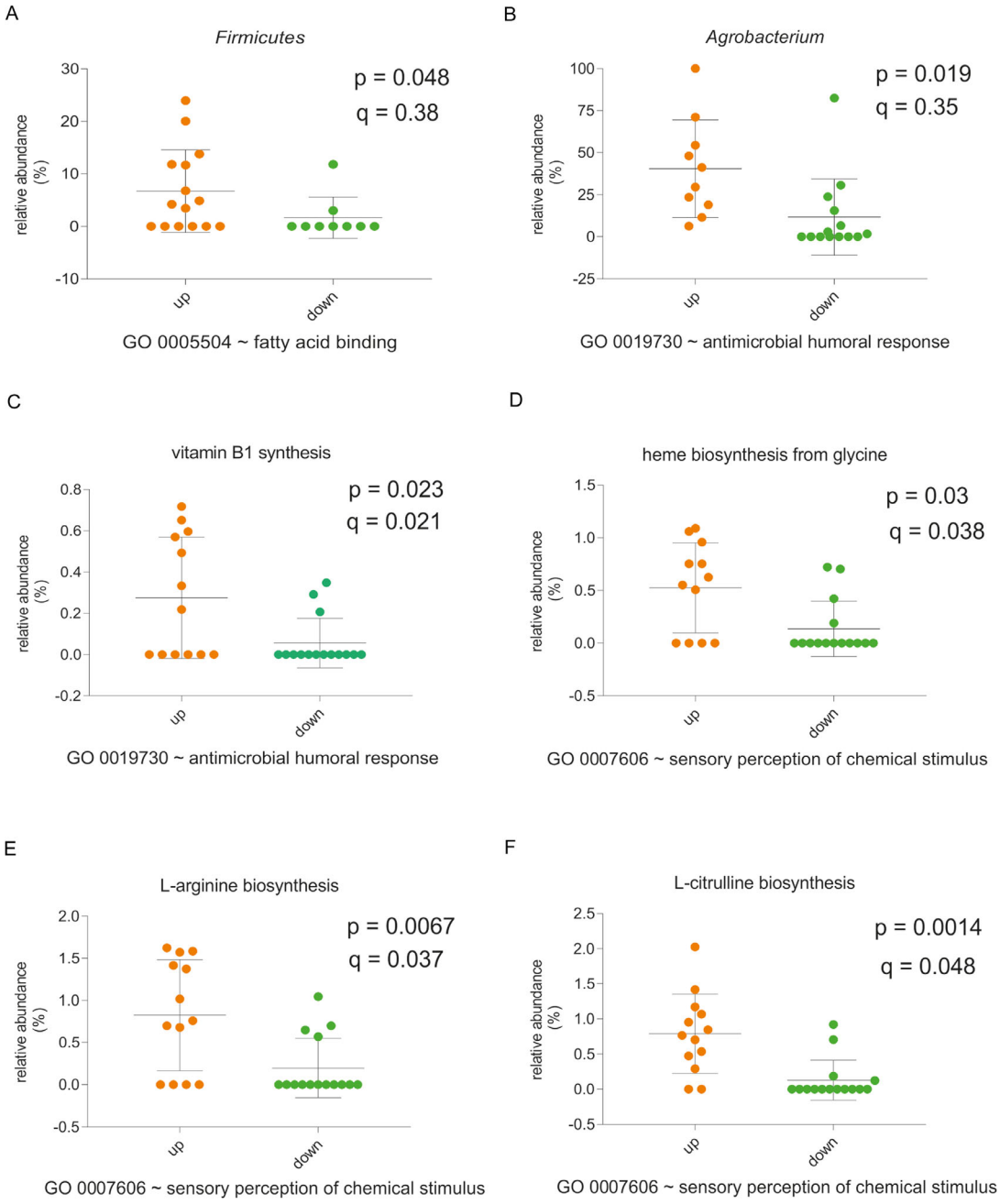

Figure 8. Associations between the ocular surface microbiome and the tear proteome. Relative abundances of taxa (**A, B**) or pathways (**C–F**) associated with up- or downregulated Gene Ontology (GO) terms (q-values after adjusting for false discovery rate, MaAsLin). Mean values and standard deviation are shown.

microbiome and the tear proteome. We used multivariate association by linear models (MaAsLin) to examine whether relative abundances of taxonomical or functional features of the microbiome were associated with regulated functional features of the proteome. A boosting step in the MaAsLin algorithm ensures that only metadata that are associated with the given taxon or pathway are included in the model, implying that all associations identified by the modeling approach have been corrected for all confounding factors. An upregulation of the GO term "fatty acid binding" positively correlated with the phylum *Firmicutes*. An upregulation of "antimicrobial humoral response" positively correlated with both, the genus *Agrobacterium* and vitamin B1 synthesis. The heme biosynthesis (from glycine), L-arginine biosynthesis, and L-citrulline biosynthesis positively correlated with an upregulation of the GO term "sensory perception of chemical stimulus" (Fig. 8).

Discussion

Although both, the human ocular microbiome and the tear proteome, may play an important role in ocular surface health and disease, the cross-talk between the two has not been investigated so far. In the present study, we

Investigative Ophthalmology & Visual Science

characterized the ocular surface microbiome as well as the tear proteome and performed association studies between the two systems in order to provide a comprehensive list of microorganisms and their functional profiles and metabolites for biomarker research of ocular surface-associated diseases.

Characteristics of the Ocular Surface Microbiome and Tear Proteome in Humans

The characterization of the ocular surface microbiome has changed dramatically over time with the introduction of modern techniques to isolate bacteria of the conjunctival surface.[27] Initial approaches using traditional microbial culture methods identified coagulase negative bacteria with *Staphylococcus aureus* and *Propionibacterium acnes* being the most abundant species on the ocular surface.[4] More recently, 16s rRNA sequencing has introduced the possibility of a more in-depth characterization of the local microbiome, especially revealing a significant greater diversity at the genus level compared to conventional cultivation techniques.[28–30] In this study, we used whole-genome shotgun sequencing which has, compared to 16s rRNA sequencing, the advantage of sequencing of all genomic DNA in a given sample, leading to a higher resolution and detection of more species,[31] also including taxa of the superkingdoms archea, viruses, and eukaryotes.[32–34] Although the ocular microbiome composition in our cohort was dominated by the phyla *Actinobacteria, Proteobacteria*, and *Firmicutes* (see Figs. 3A, 3B), *Propionibacterium*, *Agrobacterium*, and *Corynebacterium* were the most abundant genera in the cohort (see Figs. 3C, 3D). These findings are in accordance with previous studies.[6] Significant differences between lid and conjunctival samples were observed on species level with an increased abundance of *Staphylococcus epidermidis* and *Propionibacterium acnes* in lid compared to conjunctival samples (see Fig. 4C). These results can be explained by several facts, including that both, *Staphylococcus epidermidis* and *Propionibacterium acnes*, are part of the normal flora of the human skin, *S. epidermidis* is known to be a regular contaminant of swabs and that the lid itself is part of the human skin.

A further advantage of whole-metagenome shotgun compared to 16s rRNA sequencing is that the former allows a more reliable functional profiling.[32] In this study, lid microbiomes were enriched in genes of glycolysis lll, adenosine de novo biosynthesis ($P = 0.006$) and L-isoleucine biosynthesis pathways (Fig. 4D). Because most of the energy of the cornea is supplied by aerobic processes, the eye needs high amounts of oxygen and glucose.[35] As all the pathways mentioned above are involved in energy generation by aerobic processes, our results suggest that the microbiome of the lid has higher energy requirements than the conjunctiva that is, at least partially, provided by metabolic activities of microorganisms of the ocular surface microbiome.

The ocular microbiome harbors a much less diverse species variety compared to the oral and gut microbiome that, among other factors, may be explained by antimicrobial components in meibomian lipids present in human tears. In general, the composition of the latter reflects the health of the underlying tissue and thus, several attempts have been made to explore the human tear proteome to detect potential biomarkers of ocular surface health and disease, such as dry eye,[10,11] blepharitis,[8] and Sjögren's syndrome.[9] In this study, through nLC-MS/MS we quantified 2172 tear proteins and functionally classified these proteins enabling correlation studies with the profiled microbiome data. Lacrimal constituents of tears may be influenced by the ocular surface microbiome and vice versa. On the other hand, bacterial enzymes may catalyze triglycerides and cholesteryl esters found in meibomian lipids and therefore affecting its composition (see Fig. 1B).

The Ocular Surface Microbiome and Tear Proteome in Human Immune Defense

The ocular surface is constantly exposed to the environment and is vulnerable to infections due to the lack of lymphatic tissue.[36] Furthermore, infections on the ocular surface can be detrimental to vision. One of the most important functions of the tear film is the protection of the ocular surface against pathogens.[37] This function is reflected in our data as functional classification of the identified proteins revealed that many human tear proteins are involved in the biological process "antimicrobial humoral response" (see Fig. 7B). Moreover, four of the five most abundant proteins of the tear proteome (see Fig. 6A), including lactoferrin, lipocalin-1, lysozyme, and IgA, have antimicrobial activity (see Fig. 1B). Lactoferrin and lysozyme exhibit a broad spectrum of antimicrobial activity. Secretory IgA reacts with surface antigens presented on bacterial cells, thus inhibiting their adherence to the ocular surface.[38] Lipocalin-1 is crucial in ocular surface protection by solubilizing lipids and thereby stimulating the stability of the tear film and delaying the evaporation at the aqueous-lipid-air interface.[39] Moreover, mucins, the major components in the mucin layer of the human tear film, also play an important role in the maintenance of a healthy and stable ocular surface by binding to microorganisms and thereby preventing the binding of the latter to the epithelium of the ocular surface.[40] In the present study, we were able to identify 8 different mucins, including Mucin-1, Mucin-4, Mucin-5AC, Mucin-5B, Mucin-7, Mucin-16, Mucin-20, and Mucin-like protein 1. Furthermore, we identified several other tear proteins with antimicrobial activity, such as antileukoproteinase, elafin, proline-rich proteins, defensins, dermcidin, cystatins, and members of the S100 protein family (S100 A2, A4, A6, A8, A9, A10, A11, A12, A13, A16, and P, consistent with previous observation[12]). Previous studies showed that altered S100 proteins levels are associated with various diseases, including cancer and inflammatory disorders,[12] and cystatin S and SN were found to be downregulated in tears of patients with mycotic keratitis.[41] In addition to the previous reported cystatins A, B, C, D, S, N, and SN, we identified cystatin SA in human tear fluid for the first time.

As described, the composition and its functional profile of the ocular surface microbiome as well as the antimicrobial activity of many tear proteins are crucial for a healthy ocular surface. Most important, an instability in the composition of the tear film results in a disturbed defense against pathogens, favoring the onset of an imbalanced microbial composition in the eye, called dysbiosis, and, thus, ultimately leading to the development of eye diseases. This indicates the importance of the ocular surface microbiome and the tear proteome as well as the interaction between these two systems in health and disease of the underlying tissue. This is the first study performing association studies

Investigative Ophthalmology & Visual Science

between relative abundances of taxonomical as well as functional features of the ocular surface microbiome and regulated functional features of the tear proteome in humans. Using multivariate association by linear models, we showed a positive correlation between the phylum *Firmicutes* and the molecular function "fatty acid binding" (see Fig. 8A). Furthermore, Wang et al. showed that fatty acid binding proteins regulate antimicrobial functions via Toll signaling pathway,[42] providing further evidence for protection of the ocular surface against pathogens by the tear film. In addition, we showed that the upregulation of "antimicrobial humoral response" in the tear proteome positively correlated with both, the genus *Agrobacterium* and with vitamin B1 synthesis (Figs. 8B, 8C). All organisms require vitamin B1 due to its role in essential metabolic pathways, such as glycolysis.[43] Furthermore, a protective effect of vitamin B1 against oxidative damage in some tissues including the retina has been reported.[44]

The positive correlation of the biosynthesis of L-arginine and L-citrulline with an upregulation of "sensory perception of chemical stimulus" (GO 0007606) in the tear proteome (see Figs. 8E, 8F) reflects the important role of the microbial biosynthesis of specific amino acids in visual processes. This assumption is supported by the fact that the GO term "visual perception" (GO 0007601), describing the physiological process of human vision, is a child term of GO 0007606. Last, heme biosynthesis also positively correlated with an upregulated "sensory perception of chemical stimulus" (see Fig. 8D), reflecting an essential role of heme in the eye. This assumption is in accordance with previous studies demonstrating that altered heme homeostasis in endothelial cells result in impaired angiogenesis,[45] which is related to many eye diseases, such as AMD. Moreover, in human retinal microvascular endothelial cells and in animal models of ocular neovascularization, the inhibition of the heme biosynthesis blocks angiogenesis through mitochondrial dysfunction.[46,47]

Conclusions

We performed an extensive taxonomical and functional characterization of the ocular surface microbiome and a profound functional analysis of an extended list of tear proteins in humans, revealing the importance of both systems and their associations in ocular health and disease. This study may have significant impact on the development of treatment strategies, including the definition of new disease markers and thus, allowing targeted preventive care of ocular surface-associated diseases.

Acknowledgments

Declarations

Ethics Approval and Consent to Participate: This study was approved by the Ethics Committee of the Canton of Bern (ClinicalTrials.gov: NCT04656197) and all participants gave written informed consent to participate in the study.

Data Availability: The datasets supporting the conclusions of this article are available in the European Nucleotide Archive under the accession number PRJEB38989.

Supported by OPOS foundation, St. Gallen, Switzerland, and Fondation Bertarelli Catalyst Fund, EPFL (Ecole Polytechnique Fédérale de Lausanne), Lausanne, Switzerland (CF10000044 – EPFL SCR0237812).

Disclosure: **D.C. Zysset-Burri**, None; **I. Schlegel**, None; **J.-B. Lincke**, None; **D. Jaggi**, None; **I. Keller**, None; **M. Heller**, None; **S.B. Lagache**, None; **S. Wolf**, None; **M.S. Zinkernagel**, None

References

1. Turnbaugh PJ, Ley RE, Hamady M, Fraser-Liggett CM, Knight R, Gordon JI. The human microbiome project. *Nature*. 2007;449:804–810.
2. Zinkernagel MS, Zysset-Burri DC, Keller I, et al. Association of the Intestinal Microbiome with the Development of Neovascular Age-Related Macular Degeneration. *Sci Rep*. 2017;7:40826.
3. Zysset-Burri DC, Keller I, Berger LE, et al. Retinal artery occlusion is associated with compositional and functional shifts in the gut microbiome and altered trimethylamine-N-oxide levels. *Sci Rep*. 2019;9:15303.
4. Perkins RE, Kundsin RB, Pratt MV, Abrahamsen I, Leibowitz HM. Bacteriology of normal and infected conjunctiva. *J Clin Microbiol*. 1975;1:147–149.
5. Dougherty JM, McCulley JP. Comparative bacteriology of chronic blepharitis. *Br J Ophthalmol*. 1984;68:524–528.
6. Huang Y, Yang B, Li W. Defining the normal core microbiome of conjunctival microbial communities. *Clin Microbiol Infect*. 2016;22:643.e7–643.e12.
7. Green-Church KB, Butovich I, Willcox M, et al. The international workshop on meibomian gland dysfunction: report of the subcommittee on tear film lipids and lipid-protein interactions in health and disease. *Invest Ophthalmol Vis Sci*. 2011;52:1979–1993.
8. Koo BS, Lee DY, Ha HS, Kim JC, Kim CW. Comparative analysis of the tear protein expression in blepharitis patients using two-dimensional electrophoresis. *J Proteome Res*. 2005;4:719–724.
9. Tomosugi N, Kitagawa K, Takahashi N, Sugai S, Ishikawa I. Diagnostic potential of tear proteomic patterns in Sjogren's syndrome. *J Proteome Res*. 2005;4:820–825.
10. Tong L, Zhou L, Beuerman RW, Zhao SZ, Li XR. Association of tear proteins with Meibomian gland disease and dry eye symptoms. *Br J Ophthalmol*. 2011;95:848–852.
11. Zhou L, Beuerman RW, Chan CM, et al. Identification of tear fluid biomarkers in dry eye syndrome using iTRAQ quantitative proteomics. *J Proteome Res*. 2009;8:4889–4905.
12. Zhou L, Zhao SZ, Koh SK, et al. In-depth analysis of the human tear proteome. *J Proteomics*. 2012;75:3877–3885.
13. Bolger AM, Lohse M, Usadel B. Trimmomatic: a flexible trimmer for Illumina sequence data. *Bioinformatics*. 2014;30:2114–2120.
14. Langmead B, Salzberg SL. Fast gapped-read alignment with Bowtie 2. *Nature Methods*. 2012;9:357–359.
15. Segata N, Waldron L, Ballarini A, Narasimhan V, Jousson O, Huttenhower C. Metagenomic microbial community profiling using unique clade-specific marker genes. *Nature Methods*. 2012;9:811–814.
16. Human Microbiome Project Consortium. A framework for human microbiome research. *Nature*. 2012;486:215–221.
17. Abubucker S, Segata N, Goll J, et al. Metabolic reconstruction for metagenomic data and its application to the human microbiome. *PLoS Computational Biology*. 2012;8:e1002358.
18. Posa A, Brauer L, Schicht M, Garreis F, Beileke S, Paulsen F. Schirmer strip vs. capillary tube method: non-invasive methods of obtaining proteins from tear fluid. *Annals of Anatomy = Anatomischer Anzeiger: Official Organ of the Anatomische Gesellschaft*. 2013;195:137–142.

19. Gunasekera K, Wuthrich D, Braga-Lagache S, Heller M, Ochsenreiter T. Proteome remodelling during development from blood to insect-form Trypanosoma brucei quantified by SILAC and mass spectrometry. *BMC Genomics*. 2012;13:556.
20. Stéphane Dray A-BED. The ade4 Package: Implementing the Duality Diagram for Ecologists. *J Stat Softw*. 2007;22:1–20.
21. Anderson MJ. A new method for non-parametric multivariate analysis of variance. *Austral Ecol*. 2001;26:32–46.
22. Morgan XC, Tickle TL, Sokol H, et al. Dysfunction of the intestinal microbiome in inflammatory bowel disease and treatment. *Genome Biology*. 2012;13:R79.
23. Wen X, Miao L, Deng Y, et al. The Influence of Age and Sex on Ocular Surface Microbiota in Healthy Adults. *Invest Ophthalmol Visual Sci*. 2017;58:6030–6037.
24. Nattinen J, Jylha A, Aapola U, et al. Age-associated changes in human tear proteome. *Clin Proteomics*. 2019;16:11.
25. Huang da W, Sherman BT, Lempicki RA. Systematic and integrative analysis of large gene lists using DAVID bioinformatics resources. *Nature Protocols*. 2009;4:44–57.
26. Huang da W, Sherman BT, Lempicki RA. Bioinformatics enrichment tools: paths toward the comprehensive functional analysis of large gene lists. *Nucleic Acids Res*. 2009;37:1–13.
27. Zegans ME, Van Gelder RN. Considerations in understanding the ocular surface microbiome. *Am J Ophthalmol*. 2014;158:420–422.
28. Dong Q, Brulc JM, Iovieno A, et al. Diversity of bacteria at healthy human conjunctiva. *Invest Ophthalmol Vis Sci*. 2011;52:5408–5413.
29. Graham JE, Moore JE, Jiru X, et al. Ocular pathogen or commensal: a PCR-based study of surface bacterial flora in normal and dry eyes. *Invest Ophthalmol Vis Sci*. 2007;48:5616–5623.
30. Schabereiter-Gurtner C, Maca S, Rolleke S, et al. 16S rDNA-based identification of bacteria from conjunctival swabs by PCR and DGGE fingerprinting. *Invest Ophthalmol Vis Sci*. 2001;42:1164–1171.
31. Ranjan R, Rani A, Metwally A, McGee HS, Perkins DL. Analysis of the microbiome: Advantages of whole genome shotgun versus 16S amplicon sequencing. *Biochem Biophys Res Communications*. 2016;469:967–977.
32. Jovel J, Patterson J, Wang W, et al. Characterization of the Gut Microbiome Using 16S or Shotgun Metagenomics. *Front Microbiol*. 2016;7:459.
33. Norman JM, Handley SA, Baldridge MT, et al. Disease-specific alterations in the enteric virome in inflammatory bowel disease. *Cell*. 2015;160:447–460.
34. Norman JM, Handley SA, Virgin HW. Kingdom-agnostic metagenomics and the importance of complete characterization of enteric microbial communities. *Gastroenterology*. 2014;146:1459–1469.
35. Schnell D, Khaireddin R. [Corneal metabolism with contact lenses in competitive sports]. *Der Ophthalmologe: Zeitschrift der Deutschen Ophthalmologischen Gesellschaft*. 2013;110:502–510.
36. St Leger AJ, Caspi RR. Visions of Eye Commensals: The Known and the Unknown About How the Microbiome Affects Eye Disease. *BioEssays: News and Reviews in Molecular, Cellular and Developmental Biology*. 2018;40:e1800046.
37. Zhou L, Huang LQ, Beuerman RW, et al. Proteomic analysis of human tears: defensin expression after ocular surface surgery. *J Proteome Res*. 2004;3:410–416.
38. Masinick SA, Montgomery CP, Montgomery PC, Hazlett LD. Secretory IgA inhibits Pseudomonas aeruginosa binding to cornea and protects against keratitis. *Invest Ophthalmol Vis Sci*. 1997;38:910–918.
39. Careba I, Gradinaru D, Chiva A, et al. Correlations between eyelid tumors and tear lipocalin, lysozyme and lactoferrin concentrations in postmenopausal women. *J Med Life*. 2015;8:94–98.
40. Mantelli F, Argueso P. Functions of ocular surface mucins in health and disease. *Curr Opin Allergy Clin Immunol*. 2008;8:477–483.
41. Ananthi S, Chitra T, Bini R, Prajna NV, Lalitha P, Dharmalingam K. Comparative analysis of the tear protein profile in mycotic keratitis patients. *Molecular Vision*. 2008;14:500–507.
42. Wang S, Zhu Y, Li X, Wang Q, Li J, Li W. Fatty acid binding protein regulate antimicrobial function via Toll signaling in Chinese mitten crab. *Fish & Shellfish Immunology*. 2017;63:9–17.
43. Costliow ZA, Degnan PH. Thiamine Acquisition Strategies Impact Metabolism and Competition in the Gut Microbe Bacteroides thetaiotaomicron. *mSystems*. 2017;2(5):e00116–e00117.
44. Cinici E, Cetin N, Ahiskali I, et al. The effect of thiamine pyrophosphate on ethambutol-induced ocular toxicity. *Cutaneous and Ocular Toxicology*. 2016;35:222–227.
45. Petrillo S, Chiabrando D, Genova T, et al. Heme accumulation in endothelial cells impairs angiogenesis by triggering paraptosis. *Cell Death and Differentiation*. 2018;25:573–588.
46. Shetty T, Sishtla K, Park B, Repass MJ, Corson TW. Heme Synthesis Inhibition Blocks Angiogenesis via Mitochondrial Dysfunction. *iScience*. 2020;23:101391.
47. Shetty T, Corson TW. Mitochondrial Heme Synthesis Enzymes as Therapeutic Targets in Vascular Diseases. *Frontiers in Pharmacol*. 2020;11:1015.

Investigative Ophthalmology & Visual Science